Quest for Mode of Binding of 2-(4-(Dimethylamino)styryl)-1-methylpyridinium Iodide with Calf Thymus DNA

Dibakar Sahoo, Prosenjit Bhattacharya, and Sankar Chakravorti*

Department of Spectroscopy, Indian Association for the Cultivation of Science, Jadavpur, Kolkata 700032, India

Received: November 12, 2009; Revised Manuscript Received: January 8, 2010

The mode of binding of 2-(4-(dimethylamino)styryl)-1-methylpyridinium iodide (DASPMI) with calf thymus DNA as revealed from different steady state and time-resolved emission spectroscopic measurements has been reported in this paper. Fluorescence enhancement of DASPMI and its quenching by potassium iodide (KI) points to groove binding of dye with ct-DNA, rather than intercalation in the ct-DNA helix. An increase in steady state anisotropy and fluorescence lifetime hints at binding with ct-DNA. The value of binding constant from emission and association constant from circular dichroic spectrum also indicates weak binding. The strong dependence on ionic strength or salt in controlling the binding of DASPMI with ct-DNA by electrostatic interaction confirms groove binding. The high semicone angle of DASPMI in ct-DNA certainly rules out the possibility of intercalated bonding. A theoretical modeling shows that the probe is bound to ct-DNA as a crescent with a curvature of 11.35 Å, which is the previously known curvature of probe in the minor groove.

Introduction

High sensitivity of the fluorescence spectroscopy[1−8] makes fluorescence probes valuable tools in chemistry, materials science, biology,and medicine to look into the properties of environment they are associated with. Upon association with biomacromolecules, such as DNA or proteins,the emission intensity of the probe increases, and they are useful markers in genomics and proteomics, as the binding with the host molecule enhances fluorescence emission ("light-up probes").[9] Various structural and electronic factors[10] control the binding affinities and sequence specificity of small molecules toward the biomacromolecules. For the development of the effective therapeutic agents in controlling gene expression[8] the interaction of the small molecules with DNA provides valuable information. The interactions between small molecules and DNA studies help us to design new and effective drugs against the several diseases.[2] Thus the quest for new efficient probes for the fluorometric detection of DNA is on,and there is increasing interest in studying the interactions of drug and dye molecules with the various biological targets.[11]

Ionic styryl dyes are known to respond to changes in transmembrane potential by a fast electrostatic mechanism.[12−14] Among these dyes the fluorescence intensity of 2-(4-(dimethylamino)styryl)-1-methylpyridinium iodide (DASPMI) is used to measure the membrane potential of mitochondria[15,16] in living cells. Due to the sensitivity of the interesting multibond rotation (Scheme 1) involved intramolecular charge transfer property of DASPMI[17,18] to both polarity and microviscosity of the medium,[5] it is used in polymer science and in cell biology.[19−21]

Calf thymus DNA (ct-DNA) is a polymer and its DNA backbone contains alternating sugar phosphate sequence. Small molecules can bind with DNA by three dominant modes:

(1) intercalative binding, where the molecules intercalate within the nucleic acid base pairs,[22,23]

SCHEME 1: Molecular Structure of DASPMI

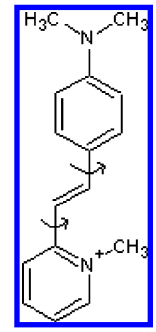

(2) electrostatic binding between the negatively charged DNA phosphate backbone and cationic or positive end of the molecules, and

(3) groove binding involving hydrogen bonding or Van der Waals interaction with the nucleic acid bases in the deep major groove or the shallow minor groove of the DNA helix.

The groove binding involves docking the thin ribbon-like molecules in the DNA minor groove, in close proximity to the sugar phosphate. Considering the enormous importance of dye−DNA interaction in designing new drugs, we intend to investigate the nature of binding of DASPMI with ct-DNA with time-resolved and steady state emission and absorption spectroscopy. Since the cationic nature of the dye might help in the binding due to electrostatic attraction with ct-DNA, in this paper we envisage throwing some light on the nature of binding as well as the way the dye docks into ct-DNA from theoretical modeling.

Experimental Section

Materials and Method. 2-(4-(Dimethylamino)styryl)-1-methylpyridinium iodide (DASPMI) was received from Aldrich Chemical and purified by vacuum sublimation. ct-DNA was purchased from Sigma-Aldrich and used without further puri-

* To whom correspondence should be addressed. E-mail: spsc@iacs.res.in. Telephone: 91-03324734971. Fax: 91-0033-24732805.

10.1021/jp910766q
Published on Web 01/20/2010

fication. NaCl and KI were obtained from SRL and were used as received. Millipore water was used throughout the experiment.

Preparation of DNA Solutions. ct-DNA stock solution was prepared by dissolving the solid material, normally at 0.3 mg mL^{-1}, in distilled water. Then, the solution was kept overnight at 4 °C. The resulting somewhat viscous solution was clear and particle-free. Working standard solutions were obtained by appropriate dilution of the stock solutions. The stock solution was stored at −20 °C. The purity of ct-DNA was verified by monitoring the ratio of absorbance at 260 nm to that at 280 nm, which was in the range 1.8−1.9. The concentration of ct-DNA was determined spectrophotometrically, using ε_{DNA} = 13 600 M^{-1} cm^{-1} at 258 nm.[24] It was observed that the complex DASPMI−nucleic acid was induced by the concentration of Na^+ ions. Due to this fact and the tendency of DASPMI to form complexes with the salts used in common buffer systems, all spectroscopic measurements were performed in Millipore water with or with out added sodium chloride. The pH of the sample solutions was adjusted by addition of small volumes of concentrated HCl or NaOH and was checked by using a digital meter.

UV/Vis Spectroscopy, Circular Dichroism, and Time Resolved Measurements. The absorption spectra at 300 K were recorded with a Shimadzu spectrophotometer (Model UV-2104 PC) and emission spectra were obtained with a Hitachi F-4500 fluorescence spectrophotometer. The concentration of DASPMI used in all fluorescence experiments was about 5×10^{-5} M, and emission was corrected for all the optical components. Steady state fluorescence anisotropy measurements were performed with a Perkin-Elmer spectrofluorometer (model-F4500) and the steady state anisotropy "r" is defined by

$$r = (I_{VV} - GI_{VH})/(I_{VV} + 2GI_{VH})$$

where I_{VV} and I_{VH} are the emission intensities obtained with the excitation polarizer oriented vertically and emission polarizer oriented vertically and horizontally, respectively. The G factor was defined as

$$G = I_{HV}/I_{HH}$$

where the intensities I_{HV} and I_{HH} now refer to the vertical and horizontal positions of the emission polarizer, with excitation polarizer being horizontal. Circular dichroism (CD) spectra were recorded on Jasco Corporation, J-815 spectrophotometer using a rectangular quartz cuvette of path length 1 cm. Spectra shown are averages of three successive scans recorded at a scan speed 50 nm/min, from which the appropriate blanks have been subtracted and the data were subjected to the noise reduction analysis. All the experiments were performed at ambient temperature (300 K) with air equilibrated solutions. Throughout the experiment, the pH of the medium was kept constant at 7.0. The fluorescence picosecond lifetime measurement was done with a Horiba Jobin Yvon Fluoro Cube 01-NL time-resolved fluorescence lifetime spectrometer with the TBX-04 detector, Data Station measurement software, and DSA6 Foundation Package, and the excitation was done at 440 nm (diode laser). The instrument response function is ~80 ps.

Molecular Modeling Studies. The crystal structure of B-DNA used for docking was extracted from the structure having Protein Data Bank[25] identifier 1DCV. The initial geometry of o-DASPMI was generated in Sybyl 6.92 (Tripos Inc.) and was minimized by the MMFF94 force field. Waters were removed from the DNA PDB file. Amber charges were added to prepare the DNA molecule for docking and the Gasteiger−Hückel method was applied to calculate the partial atomic charges for the ligands. Rotatable bonds in the ligands were assigned with Auto Dock Tools in AutoDock. Ligand docking was carried out with the AutoDock 3.0.5 Lamarckian Genetic Algorithm (GA).[26,27] In the autodocking, DNA was enclosed in the grid defined by Auto Grid having 0.375 Å spacing and 12-10 and 12-6 Lennard-Jones parameters (supplied with the program package) were used for modeling H-bonds and van der Waals interactions, respectively. Other miscellaneous parameters were assigned the default values given by the AutoDock program. The output from AutoDock was rendered with PyMol.[28]

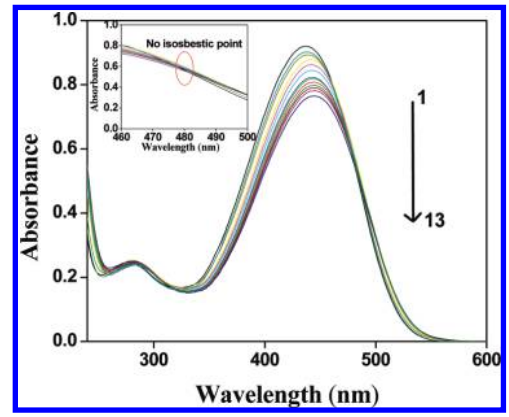

Figure 1. Absorption spectra of DASPMI in the presence of different ct-DNA concentrations. Curves correspond to 0, 2, 3, 8, 12, 17, 27, 37, 47, 60, 72, 80, and 90 μM DNA.

SCHEME 2: Energy Level Diagram for the Absorption of DASPMI upon Binding with ct-DNA

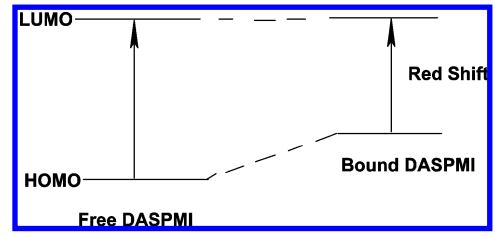

Results and Discussion

Absorption Study. DASPMI in aqueous solution shows broad unstructured lower-energy absorption bands with a maximum around 440 nm. With addition of ct-DNA to the solution, the absorbance decreases appreciably with a red shift. The absorption maximum was shifted from 440 nm for free dye to 447 nm for the bound dye in the presence of ct-DNA (Figure 1). In general, the large bathochromic shift confirms the intercalation of dye into the base stack of ct-DNA, and the small shift of 7 nm in this case could be due to the groove binding, rather than the intercalation of the dye. Here ct-DNA induced spectral changes may be explained in terms of change in local polarity around the dye, which in turn affects the stabilization of different energy levels. The polarity of the environment around the dye decreases with the addition of ct-DNA, and the energy gap between highest occupied molecular orbital (HOMO) and the lowest unoccupied molecular orbital (LUMO) of the dye decreases, which is reflected as bathochromism (Scheme 2). The absence of an isosbestic point in the absorption spectra is indicative of more than one type of binding with the dye−DNA complex.

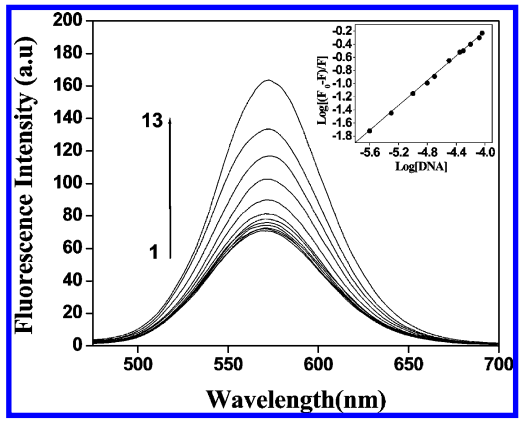

Figure 2. Emission spectra of DASPMI in the presence of different concentrations of ct-DNA. Curves correspond to 0, 2, 3, 8, 12, 17, 27, 37, 47, 60, 72, 80, and 90 μM DNA. Inset: linear plot of log $\Delta F/F$ vs DNA.

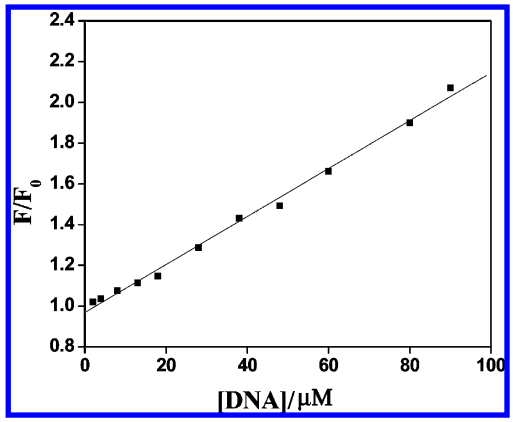

Figure 3. Stern−Volmer plot for the observed fluorescence enhancement on addition of ct-DNA to DASPMI.

Steady State Fluorescence Spectra. The fluorescence spectrum of DASPMI in aqueous solution shows a broad unstructured band around 570 nm. Addition of ct-DNA to the solution leads to the enhancement of fluorescence intensity along with a slight red shift (5 nm) (Figure 2). The observed fluorescence intensity increment points to binding interaction between the probe and ct-DNA. Binding of the dye with the ct-DNA helix hinders the rotations around various bonds and thereby decreases the possible nonradiative process through the TICT state.[29] This in turn increases the fluorescence intensity and quantum yield.

The observed fluorescence intensities were quantified by plotting F/F_0 as a function of ct-DNA concentration, where F_0 and F are the fluorescence intensity without and with ct-DNA, respectively. The plot indicates that fluorescence yields are highly sensitive to ct-DNA concentration (Figure 3). The linear plot indicates that the DASPMI fluorescence may be used as a sensitive method to determine the concentration of ct-DNA nucleotides by fluorometric methods using visible light sources for the excitation of fluorescence.

Fluorescence Quenching Study. To obtain an insight of the mode of binding of the dyes with ct-DNA, the fluorescence quenching in the ct-DNA environment was studied using potassium iodide (KI) as a quencher and the correlation between the degree of accessibility of each the molecule to the quencher and its steric bulk was examined.[30] It is well-known[31−33] that intercalation of small molecules into the ct-DNA double strands protects the entrapped molecules from an ionic quencher and consequently the fluorescence quenching of the probe due to

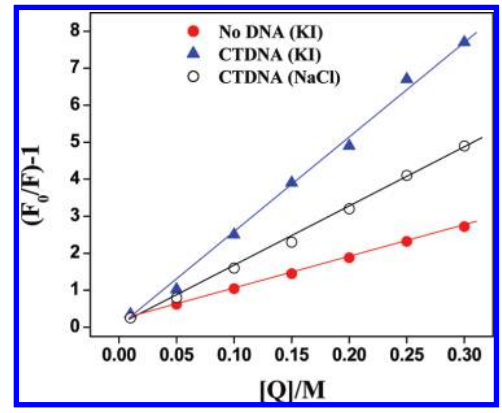

Figure 4. Quenching of DASPMI fluorescence by KI and NaCl in the presence of ct-DNA (90 μM) and by KI in the absence of ct-DNA.

an ionic quencher is not expected in an intercalated condition, whereas in electrostatic binding and groove binding the probe molecules are exposed to the approach of the quencher[32] in the aqueous phase and are likely to have no differential effect on the dye in terms of its steric bulk. Even in the groove bound situation, the negatively charged phosphate groups are expected to repel the anionic quenchers from the helix surface. In an aqueous solution, iodide anions quench the fluorescence of DASPMI very efficiently, indicating a possible groove binding. For groove binding, the effective quenching efficiency of the quencher toward the fluorophore in the ct-DNA environment is likely to be the same as that in bulk water. On the other hand, the intercalative binding of the fluorophore should lead to the reduction in the extent of fluorescence quenching in the ct-DNA environment in comparison to bulk water.[34] DASPMI fluorescence is quenched upon addition of KI in the buffer solution and also in the ct-DNA-DASPMI bound condition and the quenching phenomenon was studied following the Stern−Volmer equation

$$F_0/F = 1 + K_{SV}[Q]$$

where F_0 and F are the fluorescence intensities in the absence and presence of the quencher [Q] and K_{SV} is the Stern−Volmer quenching constant. The observed quenching constants (K_{SV}) were 8.43 and 26.16 M^{-1} in buffer solution and ct-DNA environments, respectively (Figure 4). The quenching of the dye fluorescence is in fact enhanced by a factor of more than 3 when DASPMI is bound to the helix. This enhancement of quenching may be explained on the basis of ionic strength of environment alone, which is discussed in the next section.

Effect of Ionic Strength. As the probe carries the positive charge and ct-DNA has a negative phosphate backbone, there is a significant electrostatic interaction between dyes and ct-DNA.[31,35] The effect of ionic strength on dye-DNA binding has been examined in the presence of the strong electrolyte NaCl. The increased ionic strength in the environment screens the electrostatic repulsion between the consecutive negatively charged phosphate groups[36] of ct-DNA, prompting the helix to shrink. Hence the bonding of positively charged fluorophore DASPMI and the negative phosphate group of ct-DNA gets weakened by the enhancement of the ionic strength of the solvent, which thereby helps the ct-DNA to release DASPMI from the helix[37] into the bulk solution. The free probe does not show any significant change in fluorescence spectra with addition of NaCl in buffer solution, whereas in the presence of

TABLE 1: Percent of the Dye Removed from DNA in Addition of NaCl

concentration of salt (M)	dye removed from DNA (%)
0.01	7
0.05	20
0.1	40
0.2	60
0.3	70

ct-DNA there is a sharp quenching ($K_{SV} = 16.18$) with addition of NaCl. This result indicates that quenching in the presence of ct-DNA was due to release of the probe from the ct-DNA grooves into bulk aqueous solution, in which it can undergo rapid nonradiative deactivation. We find that in the ct-DNA environment, iodide can efficiently quench the fluorescence of DASPMI ($K_{SV} = 26.16\ M^{-1}$) as compared to NaCl ($K_{SV} = 16.18$) while the quenching constant in buffer (in the presence of KI) is $K_{SV} = 8.43\ M^{-1}$ (Figure 4). So the cause of fluorescence quenching upon addition of KI is 2-fold: one is due to the breaking of the DASPMI−DNA bond and rapid nonradiative deactivation through the TICT state,[29] and the other is due to interaction of KI with DASPMI in the bulk solution. This probably accounts for the 3 times increase in quenching constant in the DASPMI−DNA bond condition, as observed earlier. Using the results in Figure 4 we can calculate the percent of the dye that is removed from the ct-DNA at each salt concentration (Table 1). So the above observation confirmed the strong dependence of the ionic strength in controlling the binding of DASPMI with ct-DNA by electrostatic interaction, which again vindicates groove binding rather than intercalation into the helix.

Equilibrium Binding Titration. To determine the binding constant (K) and binding stoichiometry (n) for the complex formation of DASPMI with ct-DNA, fluorescence titration data have been taken. Figure 2 shows the fluorescence spectrum of DASPMI in the presence of different concentrations of ct-DNA. Using this change, we can estimate the binding constant (K) and n for the binding of DASPMI to ct-DNA from the following equation[38,39]

$$\log[(F_0-F)/F] = \log K + n \log[\mathrm{DNA}]$$

where F_0 and F are the fluorescence intensities of the fluorophore in the absence and presence of different concentrations of ct-DNA, respectively.

In the case of enhancement of emission intensity, $F_0 < F$, and the above equation becomes

$$\log[(F_0-F)/F] = \log K + n \log[\mathrm{DNA}] = \log(\Delta F/F) = \log K + n \log[\mathrm{DNA}]$$

The inset of Figure 2 shows a linear plot of $\log(\Delta F/F)$ vs log[DNA], and the values of K and n are found to be 4.03×10^3 and 0.952, respectively. The value of K indicates the weak binding of the probe with ct-DNA, i.e., groove binding.

CD Study. The geometry of complex formation between ct-DNA and DASPMI is further investigated by means of circular dichroism techniques. In CD spectra no noticeable induced CD could be observed on the complex formation, indicating that DASPMI bound to ct-DNA does not possess a chiral center and is optically inactive (Figure 5). So intercalation of DASPMI may be ruled out in the binding with ct-DNA.

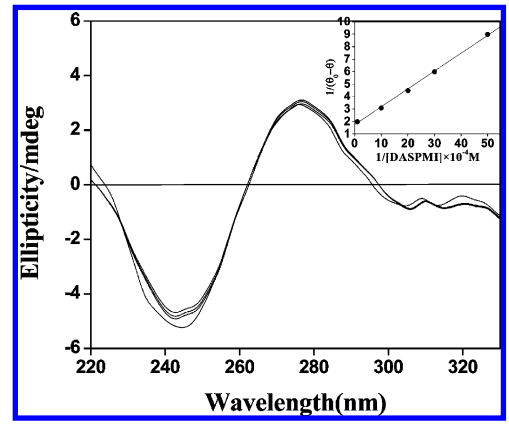

Figure 5. Circular dichroism spectrum of ct-DNA adding 2, 10, 30, and 90 μM DASPMI. Inset: linear plot for $(1/[\theta_0 - \theta])$ vs 1/[DASPMI] where θ_0 and θ are the ellipticity of DNA in the absence of DASPMI and in the presence of DASPMI, respectively.

There is a slight decrease in the positive ct-DNA dichroic signal (Figure 5), which is likely to be due to a transition from the extended nucleic acid double helix to the more compact form known as the Ψ structure.[40] The equilibrium constant of complex formation may be estimated from the change in CD response at the fixed wavelength using Benesi−Hildebrand equation[41]

$$1/\Delta A = 1/[(\varepsilon_b-\varepsilon_f)L_T] + 1/[(\varepsilon_b-\varepsilon_f)L_T K_A] \times 1/M$$

where ε is the extinction coefficient; subscripts b, f, and T denote bound, free, and total complex; and L is the concentration of DASPMI. M is the concentration of ct-DNA, and ΔA is the change of CD response at a particular wavelength. The value of the association constant (K_a) for the complex formation calculated from the slope of the double reciprocal plot (inset Figure 5) using the above equation was found to be 5.76×10^3, and the value of K_a is very much comparable to the binding constant calculated from the UV−vis study.

Steady State Anisotropy. Steady state fluorescence anisotropy gives significant information about the nature and physical characteristics of biological probes. In the anisotropy value many things, like change in size, shape, and segmental flexibility of the molecule, are reflected.[30] So the anisotropy monitoring helps us in finding the probable location of a probe in a microheterogeneous environment like micelles, reverse micelles, proteins, and DNA.[42−44] There is a sharp increase in fluorescence anisotropy with the increase in the concentration of ct-DNA, which suggests that the fluorophores are trapped in a motionally restricted region within ct-DNA compared to that in buffer water. Figure 6 also shows that the anisotropy levels off at 0.2, which indicates that, irrespective of the extent of groove binding, the overall tumbling motion of he dye−DNA complex is also responsible for the fluorescence anisotropy.

Fluorescence Lifetime. The decay of DASPMI in buffer solution may be fitted as biexponential functions with time constants 0.6 and 1.4 ns. With the addition of ct-DNA, the fluorescence decay shows biexponential behavior (Table 2), but the values of decay constants and relative amplitude 0.65 ns (0.13) and 2.7 ns (0.87) change drastically (Figure 7). Biexponential fitting is the best fitting according to the residuals (Figure 7). So after addition of ct-DNA the lifetime of the dye increases due to the binding with ct-DNA.

Molecular Modeling of DASPMI−DNA Interaction. Molecular docking studies provide some insight into the interactions

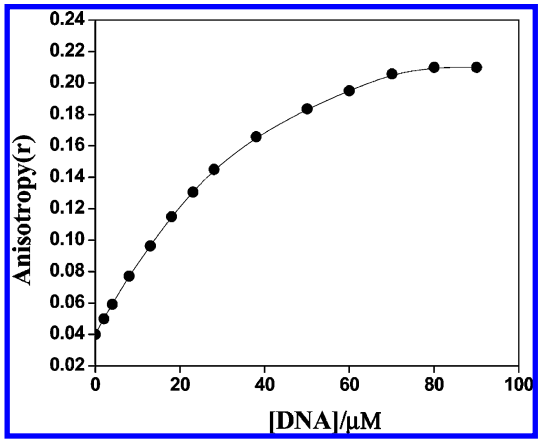

Figure 6. Variation of fluorescence anisotropy as a function of increasing concentration of ct-DNA for DASPMI. [DASPMI] = 5×10^{-5}.

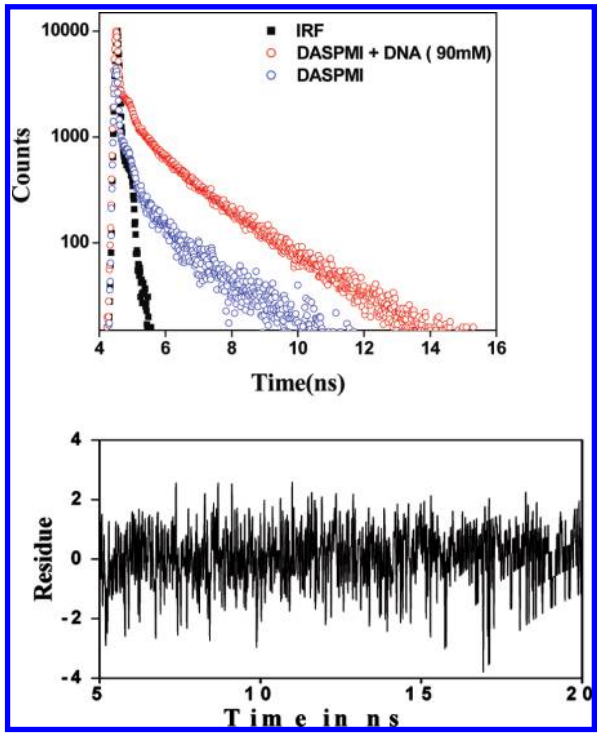

Figure 7. Time resolved fluorescence decay of DASPMI without and with DNA ([DNA] = 90 μM) and percent residuals. (IRF = instrument response function).

TABLE 2: Fitted Fluorescence Decay of DASPMI in Various Environments

systems	τ_1 (ns)	a_1	τ_2 (ns)	a_2	χ^2
water (pH = 7.0)	0.6 ± 0.02	0.68	1.4 ± 0.03	0.29	0.98
ct-DNA	0.65 ± 0.01	0.13	2.7 ± 0.02	0.87	0.99

between the macromolecule and ligand, which can corroborate the experimental results. Though the crystal structure of the complex can provide details of the interactions, general observations may be obtained from docking studies. The docking study confirms that only one conformation is possible. The docked conformation (Figure 8) shows that the DASPMI molecule exists in a crescent shape, which is similar to the curvature of probe of B-DNA.[45,46] The distance between the points of attachment with DNA (11.5 Å) is smaller than the length of the molecule

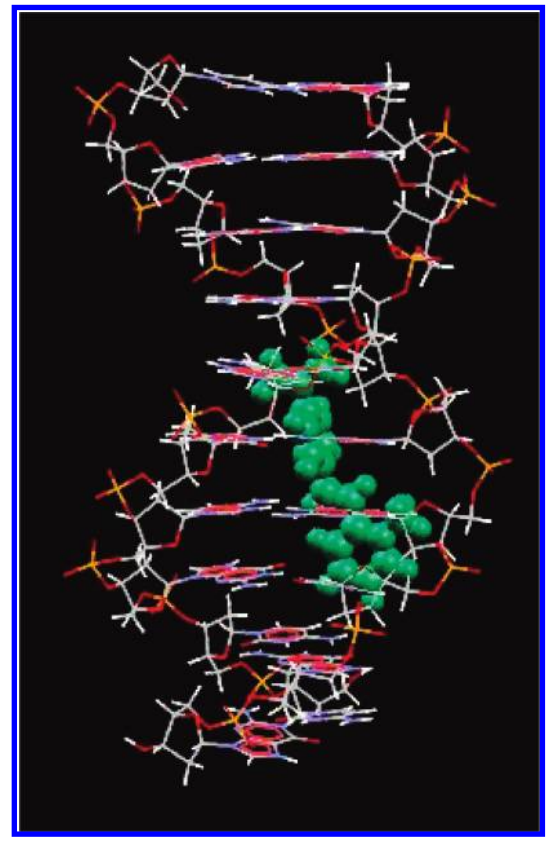

Figure 8. Docked pose of DASPMI bound to the minor groove of ct-DNA.

(14 Å), which causes the molecule to take the curved shape, and the radius of curvature of DASPMI was calculated to be 11.35 Å, which is very similar to the values of known minor groove binding agents.[47] The estimated docking energy is computed to be −13.5 kcal mol^{-1}. Minor groove binders generally have aromatic rings connected by single bonds that allow for torsional rotation to fit into the narrower helical curvature of the groove comprising the A−T region with displacement of water molecules. The extensive van der Waals contacts between the docked DASPMI and the floor and walls of the minor groove point out the significant solubilization of the complex through this interaction.

Wobbling Motion. To study the wobbling motion of dye in DNA, we applied the wobbling-in-cone model[48,49] to the temporal anisotropy of grooved bounded dye. According to this model, the rotational anisotropy decay function is denoted as

$$r(t) = r_0\left[\beta \exp\left(\frac{-t}{\tau_{slow}}\right) + (1 - \beta)\exp\left(\frac{-t}{\tau_{fast}}\right)\right]$$

where $S^2 = \beta$ is the generalized order parameter that describes the degree of restriction on the wobbling in cone orientational motion. S^2 satisfies the inequality $0 \le S^2 \le 1$, where $S^2 = 0$ describes unrestricted reorientation and $S^2 = 1$ for no wobbling in cone orientational motion.

Here faster rotational relaxation with the shorter rotational time constant τ_{fast} is described as the motion of restricted rotator (probe) having its translational dipole moment undergoing orientational diffusion within a semicone of angle θ_ω about an imaginary axis. Thus faster and slower rotational lifetime constants can be written as $1/\tau_\omega = 1/\tau_{fast} - 1/\tau_{slow}$, where τ_ω is the decay time constant associated with wobbling motion of the probe.

TABLE 3: Temporal Fluorescence Anisotropy Decay Data for DASPMI in Various Environments

system	τ_{a1} (ps)	a_1	τ_{a2} (ps)	a_2	r_0	τ_ω (ns)	θ_ω (deg)
water (pH = 7.0)	120 ± 10	1			0.39		
ct-DNA	150 ± 10	0.59	5200 ± 20	0.41	0.36	0.154	42.5

Again the semicone angle θ_ω is obtain from the order parameter as follows: $S^2 = [1/2(\cos\theta_\omega)(1 + \cos\theta_\omega)]^2$.

For $\theta_\omega \leq 30°$, the wobbling-in-cone diffusion constant D_ω is given by $D_\omega \approx 7\theta_\omega^2/24\tau_\omega$, with θ in radians.

However for $\theta_\omega \geq 30°$ and all θ_ω the D_ω is given by

$$D_\omega\tau_\omega(1 - S^2) = -x^2(1 + x)^2[\log\{(1 + x)/2\} + (1 - x)/2]/\{2(1 - x)\} + (1 - x)(6 + 8x - x^2 - 12x^3 - 7x^4)/24$$

where $x = \cos\theta_\omega$.

From Table 3 it is evident that anisotropy time is slower in ct-DNA than in other environments. The slower anisotropy time constant of 5.2 ns in ct-DNA may be due to the local thumbing of ct-DNA segments (Figure 9). Here we cannot expect the lateral diffusion of DASPMI along the DNA−water interface as all the probe molecules bind with ct-DNA with groove binding at the saturation level. The semicone angle of DASPMI in the ct-DNA environment is larger than that in other environments because the twisting motion of the ct-DNA chain combined with the internal wobbling of the dye produces a large semicone angle. Here we find the semicone angle of DASPMI (42.5°) is much larger than that for the intercalated ethidium bromide (15°)[50] in DNA, which certainly rules out the possibility of intercalated bonding in the present case. So it is expected that DASPMI is bound to ct-DNA as a groove binder. This is amply corroborated by the same type of evidence of groove binding from the previous different experimental and theoretical modeling studies.

Conclusion

The different emission spectroscopic studies confirm the binding of the dye with ct-DNA as a groove binding, rather than the other option of intercalation in the DNA helix, and it is amply corroborated by theoretical modeling of probe−DNA binding. The steric constraints imposed on the dye owing to groove binding of DASPMI with DNA restrict the rapid nonradiative deactivation in the excited state, resulting in enhanced fluorescence yields and longer fluorescence lifetime. The increased fluorescence intensity of DASPMI bound with DNA compared to that in buffer suggests that the dye could be used as DNA staining agent.

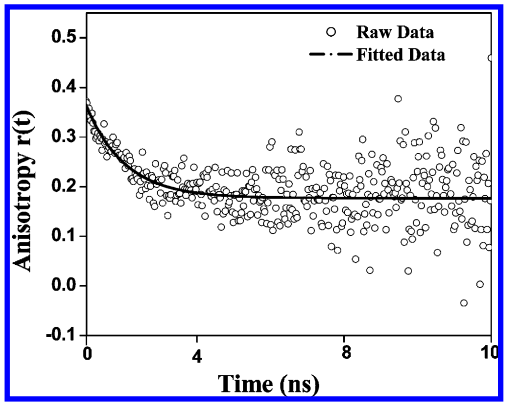

Figure 9. Temporal anisotropy decay curve of DASPMI in ct-DNA ([DNA] = 90 μM).

Acknowledgment. We thank Mr. Subrata Das, Department of Spectroscopy, IACS, for taking picosecond time-resolved data.

References and Notes

(1) *Optical Sensors*; Wolfbeis, O. S., Ed.; Springer-Verlag: Heidelberg, 2004.
(2) Mohr, G. J. *Chem.—Eur. J.* **2004**, *10*, 1082–1090.
(3) Pu, L. *Chem. Rev.* **2004**, *104*, 1687–1716.
(4) Martinez-Manez, R.; Sancenon, F. *Chem. Rev.* **2003**, *103*, 4419–4476.
(5) Valeur, B. *Molecular Fluorescence: Principles and Applications*; Wiley-VCH: Weinheim, 2002.
(6) Wiskur, S. L.; Ait-Haddou, H.; Anslyn, E. V.; Lavigne, J. *J. Acc. Chem. Res.* **2001**, *34*, 963–972.
(7) de Silva, A. P. H.; Gunaratne, Q.; Gunnlaugsson, T.; Huxley, A. J. M.; McCoy, C. P.; Rademacher, J. T.; Rice, T. E. *Chem. Rev.* **1997**, *97*, 1515–1566.
(8) Wahl, M.; Koberling, F.; Patting, M.; Rahn, E. H. *Curr. Pharm. Biotechnol.* **2004**, *5*, 299–308.
(9) Prentø, P. *Biotech. Histochem.* **2001**, *76*, 137–161.
(10) Haugland, R. G. *Handbook of Fluorescent Probes and Research Products*, 9th ed.; Molecular Probes Inc: Eugene, OR, 2002.
(11) Osborne, S. E.; Ellington, A. D. *Chem. Rev.* **1997**, *97*, 349–370.
(12) Loew, L. M.; Bonneville, G. W.; Surow, J. *Biochemistry* **1978**, *17*, 4065–4071.
(13) Loew, L. M.; Scully, S.; Simpson, L.; Waggoner, A. S. *Nature* **1979**, *281*, 497–499.
(14) Loew, L. M.; Simpson, L. L *Biophys. J.* **1981**, *34*, 353–365.
(15) Bereiter-Hahn, J. *Biochim. Biophys. Acta* **1976**, *423*, 1–14.
(16) Bereiter-Hahn, J.; Seipel, K. H.; Vö th, M.; Ploem, J. S. *Cell Biochem. Funct.* **1983**, *1*, 147–155.
(17) Strehmel, B.; Seifert, H.; Rettig, W. *J. Phys. Chem.B* **1997**, *101*, 2232–2243.
(18) Strehmel, B.; Rettig, W. *J. Biomed. Opt.* **1996**, *1*, 98–109.
(19) Spooner, S. P.; Whitten, D. G. In *Photochemistry in Organized &Constrained Media*; Ramamurthy, V., Ed.; Wiley-VCH: Weinheim, Germany, 1991; pp 691−739.
(20) Ulmann, A. *An Introduction to Ultrathin Organic Films: From-Langmuir-Blodgett to Self- Assembly*; Academic Press: San Diego, CA, 1991; Chapters 3 and 5.
(21) Ephardt, H.; Fromherz, P. *J. Phys. Chem.* **1991**, *95*, 6792–6797.
(22) Armitage, B. *Chem. Rev.* **1998**, *98*, 1171–1200.
(23) Erkkila, K. E.; Odom, R. T.; Barton, J. K. *Chem. Rev.* **1999**, *99*, 2777–2795.
(24) Gaballah, S. T.; Collier, G.; Netzel, T. L. *J. Phys. Chem. B* **2005**, *109*, 12175–12181.
(25) Berman, H. M.; Westbrook, J.; Feng, Z.; Gilliland, G.; Bhat, T. N.; Weissig, H.; Shindyalov, I. N.; Bourne, P. E. *Nucleic Acids Res.* **2000**, *28*, 235–242.
(26) Morris, G. M.; Goodsell, D. S.; Halliday, R. S.; Huey, R.; Hart, W. E.; Belew, R. K.; Olson, A. J. *J. Comput. Chem.* **1998**, *19*, 1639–1662.
(27) Morris, G. M.; Goodsell, D. S.; Huey, R.; Olson, A. J. *J. Comput.-Aided Mol. Des.* **1996**, *10*, 293–304.
(28) DeLano, W. L. *The PyMOL Molecular Graphics System*; DeLano Scientific: San Carlos, CA, 2004; http://pymol.sourceforge.net.
(29) Ramadass, R.; B-Hahn, J *J. Phys. Chem. B* **2007**, *111*, 7681–7690.
(30) Lakowicz, J. R. *Principles of Fluorescence Spectroscopy*; Plenum Press: New York, 1999.
(31) Chuan, D.; Yu-xia, W.; Yan-li, W. *J. Photochem. Photobiol. A: Chem.* **2005**, *174*, 15–22.
(32) Lerman, L. S. *J. Mol. Biol.* **1961**, *3*, 18–30.
(33) Berman, H. M.; Young, P. R. *Annu. Rev. Biophys. Bioeng.* **1981**, *10*, 87–114.
(34) Kumar, C. V.; Asuncion, E. H. *J. Chem. Soc., Chem. Commun.* **1992**, *6*, 470–472.
(35) Cao, Y.; He, X. W. *Spectrochim. Acta, Part A* **1998**, *54*, 883–892.
(36) Modukuru, N. K.; Snow, K. J.; Perrin, B. S.; Kumar, C. V. *J. Phys. Chem. B* **2005**, *109*, 11810–11818.
(37) Manning, G. S. *Acc. Chem. Res.* **1979**, *12*, 443–449.

(38) Feng, X. Z.; Lin, Z.; Yang, L. J.; Wang, C.; Bai, C. L. *Talanta* **1998**, *47*, 1223–1229.
(39) Barik, A.; Priyadarsini, K. I.; Mohan, H. *Photochem. Photobiol.* **2003**, *77*, 597–603.
(40) Jordan, C.; Lerman, L.; Venable, J. *Nature* **1982**, *236*, 67–70.
(41) Benesi, H. A.; Hildebrand, J. H. *J. Am. Chem. Soc.* **1949**, *71*, 2703–2707.
(42) Mallick, A.; Haldar, B.; Chattopadhyay, N. *J. Photochem. Photobiol. B: Biol.* **2005**, *78*, 215.
(43) Sahoo, D.; Chakravorti, S. *J. Photochem. Photobiol. A: Chem.* **2009**, *205*, 129–138.
(44) Mallick, A.; Haldar, B.; Maiti, S.; Chattopadhyay, N. *J. Colloid Interface Sci.* **2004**, *278*, 215–223.
(45) Reddy, B. S.; Sondhi, S. M.; Lown, J. W. *Pharmacol. Ther.* **1999**, *84*, 1–111.
(46) Neidle, S. *Nat. Prod. Rep.* **2001**, *18*, 291–309.
(47) Slickers, P.; Hillebrand, M.; Kittler, L.; Lober, G.; Suhnel, J. *Anti-Cancer Drug Des.* **1998**, *13*, 463–488.
(48) Lipari, G.; Szabo, A. *Biophys. J.* **1980**, *30*, 489–506.
(49) Wang, C. C.; Pecora, R. *J. Chem. Phys.* **1980**, *72*, 5333−5340.
(50) Millar, D. P.; Robbins, R. J.; Zewail, A. H. *Proc. Natl. Acad. Sci. U.S.A.* **1980**, *77*, 5593–5597.

JP910766Q